Dalitz decay studies at BESIII *

Dayong Wang[1;1)](for BESIII Collaboration)

[1] School of Physics and State Key Lab. of Nucl. Phys. and Tech., Peking University, Beijing 100871, China

Abstract: EM Dalitz decays could be sensitive and provide very rich information about meson structures, and plays an important role in constraining the uncertainties to $(g-2)_\mu$. BESIII has performed and published several Dalitz decays,including $\eta' \to \gamma e^+e^-$, $J/\psi \to Pe^+e^-(P = \eta', \eta, and\ \pi^0)$, $\eta' \to \omega e^+e^-$ etc.. These processes are all observed and measured for the first time. They have furthered our knowledge about meson structures and meson interactions. Many more related work is ongoing. There will be more results to come, and they will further test the theory against the measurements and could be sensitvie to the new physics beyond the standard model.

Key words: BESIII, Dalitz Decay, Meson Structure, Vector Meson Dominance

PACS: 12.40.Vv, 13.20.-v, 13.40.Gp, 13.40.Hq,

1 Introduction

BEPCII is the only currently running τ-charm factory working at the C.M.energy range of 2.0-4.6GeV, located at Institute of High Energy Physics, Beijing. This energy range has a lot of unique features which benefit greatly the rich physics programs:

- It is rich of resonances, including many charmonia and charmed mesons.
- Pairs of particles, such as τ, D, D_s, charmed baryons etc are copiously produced with unique threshold characteristics.
- This energy region is in the transition between perturbative and non-perturbative in terms of QCD.
- Different types of hadrons, conventional or exotic, can demonstrate their structures and interactions through processes of their productions, decays, transitions and behaviors under various probes.

The BESIII detector has a geometrical acceptance of 93% of 4π and consists of four main components: (1)A small-celled, helium-based main draft chamber (MDC) with 43 layers, which provides measurements of ionization energy loss (dE/dx). The average single wire resolution is 135 μm, and the momentum resolution for charged particles with momenta of 1 GeV/c in a 1 T magnetic field is 0.5%. (2)An electromagnetic calorimeter (EMC) made of 6240 CsI (Tl) crystals arranged in a cylindrical shape (barrel) plus two end caps. For 1.0 GeV photons, the energy resolution is 2.5% in the barrel and 5% in the end caps, and the position resolution is 6 mm in the barrel and 9 mm in the end caps. (3) A time-of-flight system for particle identification (PID) composed of a barrel part made of two layers with 88 pieces of 5 cm thick, 2.4 m long plastic scintillators in each layer, and two end caps with 96 fan-shaped, 5 cm thick plastic scintillators in each end cap. The time resolution is 80 ps in the barrel and 110 ps in the endcaps, corresponding to a $2\sigma K/\pi$ separation for momenta up to about 1.0 GeV/c. (4) A muon chamber system(MUC) made of about 1000 m^2 of resistive plate chambers arranged in nine layers in the barrel and eight layers in the end caps, and incorporated in the return iron of the superconducting magnet. The position resolution is about 2 cm.More details of the detector are described in Ref [3].

In general, the clean environments and high luminosity at BESIII are very helpful to study the structure and interaction of hadrons. BESIII has accumulated 1.3 Billion J/Ψ's, 0.5 Billion Ψ''s and $2.9fb^{-}1$ at $\Psi(3773)$, all of which are the largest data sets in the world. There are also very huge samples of light mesons from decays of these charmonia, such as η, η', π^0, K etc. By simple estimation based on the branching ratios, there would be about 7.1M η''s and 1.9M η''s from the two most abundant channels in the J/Ψ sample, which provide ideal samples for studying their Dalitz decays.

2 Dalitz decay of mesons and experimental techniques

Meson Dalitz decays are very sensitive EM probes to study the structures and the interactions of mesons [2]. The information of meson transition form factors(TFF)

Received 28 Nov. 2015

∗ Supported by Joint Funds of the National Natural Science Foundation of China(U1232105) and by Ministry of Science and Technology(2015CB856700)

1) E-mail: dayong.wang@pku.edu.cn

etc can be retrieved from these processes to test various models of mesons. These TFFs can also help to reduce the uncertainties caused by the light-by-light hadronic contributions to the calculations of $(g-2)_\mu$, which has seen 3.6σ discrepancies with the experimental measurements [4, 5].

There are a pair of electron and positron in the final states of meson Dalitz decays, which could be easily polluted by the converted electron-positron pairs from phontons interacting with detector materials. Thus it is crucial to exclude the gamma conversion events as much as possible in order to establish the meson Dalitz decays experimentally.

At BESIII, a photon conversion finder is developed, with the algorithm based on the information of common vertex position on the tranverse plane. It is described in Ref [6].

Fig. 1 shows the performance of vetoing gamma conversions, with the process $J/\psi \to \eta'\gamma, \eta' \to \gamma\pi^+\pi^-$. The conversion mostly takes place at beam pipe and the inner MDC wall. The algorithm can reconstruct the conversion vertex quite well and data-MC consistency is good.

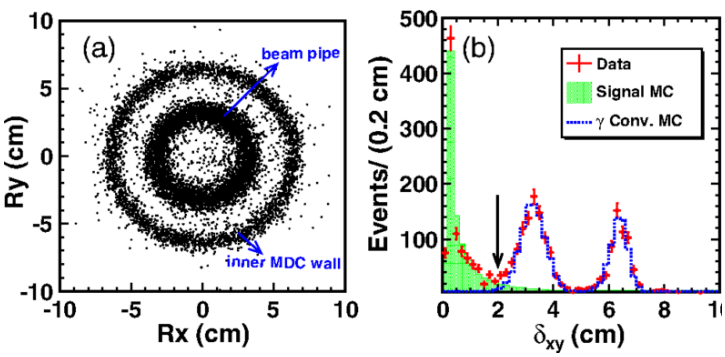

Fig. 1. Veto of gamma conversions at BESIII. (a) R_y vs R_x distributions for the simulated gamma conversion events. (b)δ_{xy} distributions. The (green) shaded histogram shows the MC-simulated signal events. The (red) dots with error bars are data. The (blue) dotted histogram shows the background from the gamma-conversion events. In (b), the solid arrow indicates the requirement on δ_{xy}.

The ratio $R_{\eta'}$ can be described clearly in theory. It is formulated with the calculable QED part for a point meson, then times the TFF. The latter is described by phenomenological models, and can be experimentally determined from differences between the measured dilepton invariant mass spectrum and the QED calculation. In the vector meson dominance (VMD) model [2], it is assumed that interactions between a virtual photon and hadrons are dominated by a superposition of neutral vector meson states. So we could retrieve the TFF information from the measurements. Fig 2 shows the efficiency-corrected signal yields versus mass of electron positron pairs from $\eta' \to \gamma e^+e^-$, with the QED shape superimposed for comparison. The discrepancy between QED and data, which reflects the TFF, is evident in the high M(ee) region.

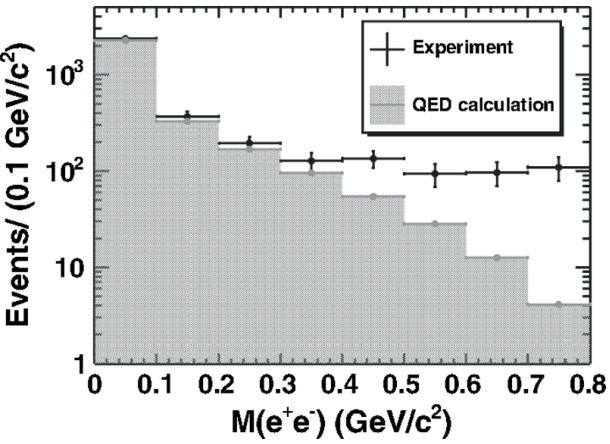

Fig. 2. Efficiency-corrected signal yields versus mass of electron positron pairs from $\eta' \to \gamma e^+e^-$. The (black) crosses are data and the (gray) shaded histogram indicates the pointlike QED result

3 First observation of $\eta' \to \gamma e^+e^-$

BESIII measured the Dalitz decay $\eta' \to \gamma e^+e^-$ for the first time. The results are published at [7].The differential decay width, are normalized to the radiative decay width $\Gamma(\eta' \to \gamma\gamma)$ to reduce the common systematic errors. The measured ratio is $R_{\eta'} = (2.13 \pm 0.09(stat) \pm 0.07(sys)) \times 10^{-2}$. This corresponds to a branching fraction $BR(\eta' \to \gamma e^+e^-) = (4.69 \pm 0.20(stat) \pm 0.23(sys)) \times 10^{-4}$. The first errors are statistic and the second ones are systematic.

The most common TFF model uses only the first term in the dispersion relation. The results of a least-squares fit with this single-pole model are shown in Fig. 3. The parameters of the form factors thus determined are in agreement with the result obtained in the process of $\eta \to \gamma\mu^+\mu^-$ as measured in [10].

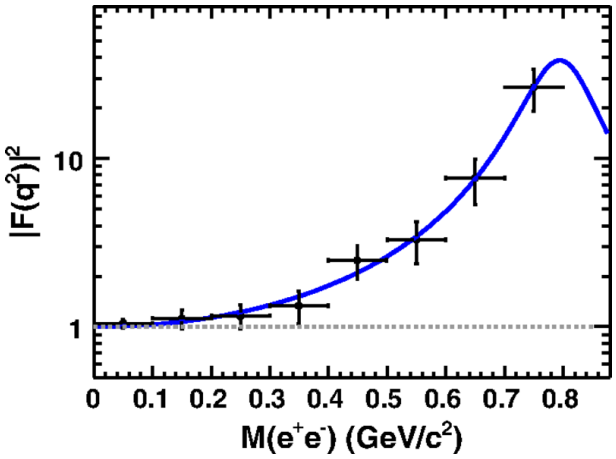

Fig. 3. The single-pole form factor fitting of $\eta' \to \gamma e^+e^-$. The (black) crosses are data, where the statistical and systematic uncertainties are combined; the (blue) solid curve shows the fit results. The (gray) dotted line shows the pointlike case for comparison.

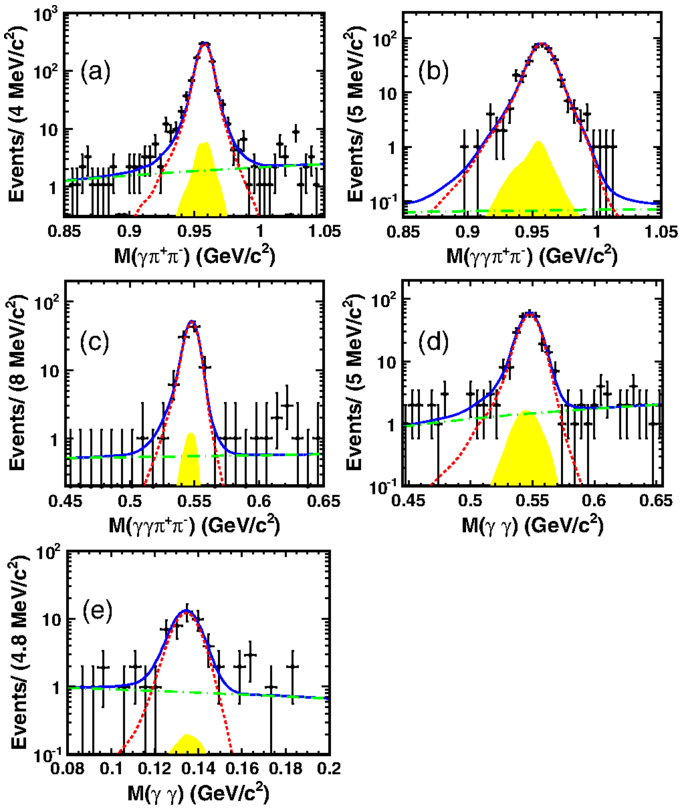

Fig. 4. Mass distributions of the pseudoscalar meson candidates in $J/\psi \to Pe^+e^-$. The subplots (a) to (e) are from different pseudoscalar states and their subsequent decay channels as inidcated. The (black) dots with error bars are data, the (red) dashed lines represent the signal, the (green) dotted-dashed curves show the nonpeaking background shapes, and the (yellow) shaded components are the shapes of the peaking backgrounds from the $J/\psi \to Pe^+e^-$ decays. Total fits are shown as the (blue) solid lines

4 First observation of $J/\psi \to Pe^+e^-(P = \eta', \eta, and\ \pi^0)$

In the previous measurements from other experiments, only Dalitz decays of light mesons are studied. In order to shed light on some of the puzzles observed in these measurements, it would be interesting to search and study the Dalitz decay of heavy quarkonium.

The theoretical and experimental investigations of the EM Dalitz decays of the light vector mesons motivate us to study the rare charmonium decays $J/\psi \to Pe^+e^-$, which should provide useful information on the interaction of the charmonium states with the electromagnetic field. The huge J/ψ sample at BESIII provides a good chance for this. BESIII made this measurement and provided experimental information on these decays for the first time [8].

BESIII studied the processes of $J/\psi \to Pe^+e^-$, and established this decay patterns for three different pseudoscalar mesons: η', η, and π^0 in the major decay modes. Fig. 4 shows the mass distributions of the pseudoscalar meson candidates in $J/\psi \to Pe^+e^-$. All the modes are established experimentally for the first time.

The branching fractions of these processes are determined. The BR are measured to be $B(J/\psi \to \eta' e^+e^-) = (5.81 \pm 0.16 \pm 0.31) \times 10^{-5}$, $B(J/\psi \to \eta e^+e^-) = (1.16 \pm 0.07 \pm 0.06) \times 10^{-5}$, and $B(J/\psi \to \pi^0 e^+e^-) = (7.56 \pm 1.32 \pm 0.50) \times 10^{-7}$ respectively.

The measurements for $J/\psi \to \eta' e^+e^-$ and $J/\psi \to \eta e^+e^-$ decay modes are consistent with the theoretical prediction in Ref. [11]. The theoretical prediction for the decay rate of $J/\psi \to \pi^0 e^+e^-$ based on the VMD model is about 2.5 standard deviations from the measurement in this analysis, which may indicate that further improvements of the QCD radiative and relativistic corrections are needed.

Direct information on the form factor is obtained by studying the efficiency-corrected signal yields for each given $M(e^+e^-)$ bin. Fig. 5 shows the form factor obtained for $J/\psi \to \eta' e^+e^-$. The crosses are data, and the fit is shown as the (blue) solid curve. The (red)

dotted-dashed curve indicate the prediction of the simple pole model, where the form factor is parametrized by the simple pole approximation with the pole mass at 3.686 GeV/c^2.

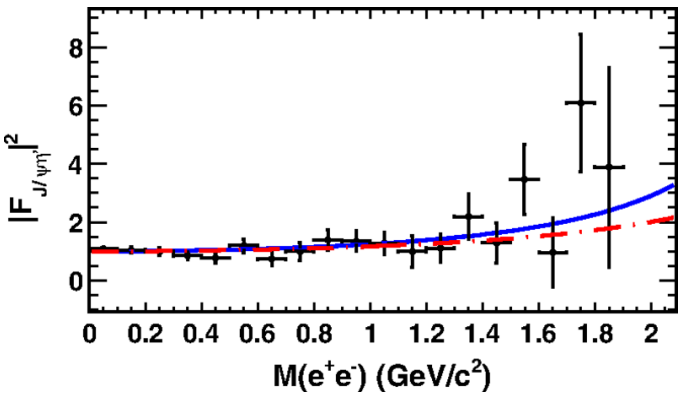

Fig. 5. Form factor for $J/\psi \to \eta' e^+ e^-$. The crosses are data, the (red) dotted-dashed curve is the prediction of the simple pole model with the pole mass of 3.686 GeV/c^2, and the fit is shown as the (blue) solid curve.

5 Measurement of $\eta' \to \omega e^+ e^-$

With a sample of 1.31 billion J/ψ events collected with the BESIII detector, we have also analyzed the decays $\eta' \to \gamma\omega$ and $\eta' \to \omega e^+ e^-$, via $J/\psi \to \eta'\gamma$. The results are published at [9].

Similar to the study of $\eta' \to \gamma e^+ e^-$, the process $\eta' \to \omega e^+ e^-$ has to be measured with respect to the normalization process of $\eta' \to \omega\gamma$. With the optimized event selections, the decay $\eta' \to \omega\gamma$ is observed in the dis tribution of $M(\pi^0\pi^+\pi^-\gamma)$ versus $M(\pi^0\pi^+\pi^-)$ shown in Fig. 6. The concentration of events in the central region indicate the existence of $\eta' \to \omega\gamma$, which serves as normalization.

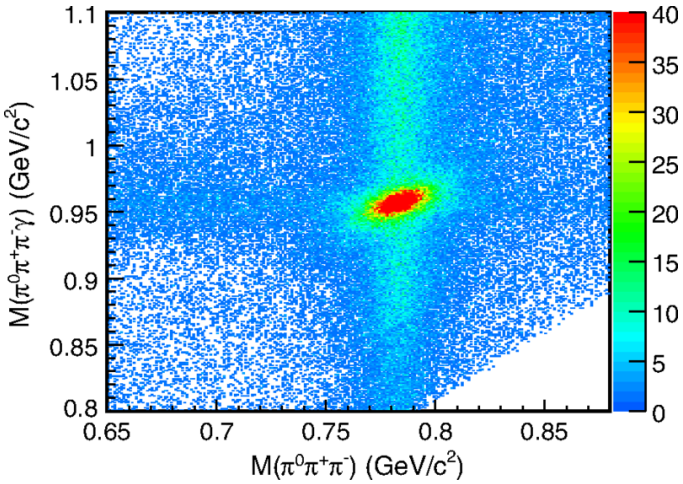

Fig. 6. 2d distribution of the invariant masses $M(\pi^0\pi^+\pi^-\gamma)$ vs $M(\pi^0\pi^+\pi^-)$ from from $\eta' \to \omega e^+ e^-$ data.

To improve the mass resolution, as well as to better handle the background in the vertical band around the ω mass region and horizontal band around the η' mass region, we determine the signal yield from the distribution of the difference between $M(\pi^0\pi^+\pi^- e^+ e^-)$ and $M(\pi^0\pi^+\pi^-)$. The backgrounds in the vertical and horizontal bands do not peak in the signal region, which is demonstrated by the inclusive MC sample, as shown by the histogram in Fig. 7.

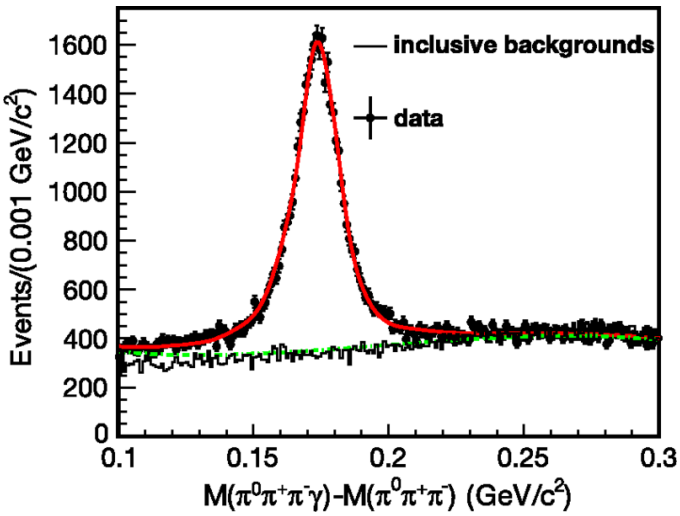

Fig. 7. Distribution of the mass difference $M(\pi^0\pi^+\pi^- e^+ e^-) - M(\pi^0\pi^+\pi^-)$ from from $\eta' \to \omega e^+ e^-$. The dots with error bars are data, the histogramshows theMC simulation of inclusive J/ψ decays. The solid curve represents the fit results, and the dashed curve is the background determined by the fit.

To determine the $\eta' \to \omega e^+ e^-$ yield, an unbinned maximum likelihood fit to on the distribution of $M(\pi^0\pi^+\pi^- e^+ e^-) - M(\pi^0\pi^+\pi^-)$, as shown in Fig. 8, is performed. The signal component is modeled by the MC simulated signal shape convoluted with a Gaussian function to account for the difference in the mass resolution between data and MC simulation. The shape of the dominant non-resonant background is derived from the MC simulation, and its magnitude is fixed taking into account the decay branching fraction from the PDG [1]. The remaining background contributions are described with a 2nd-order Chebychev polynomial. The fit shown in Fig. 8 has a statistical significance of 8 σ, which is determined by the change of the log-likelihood value and of the number of degrees of freedom in the fit with and without the signal included.

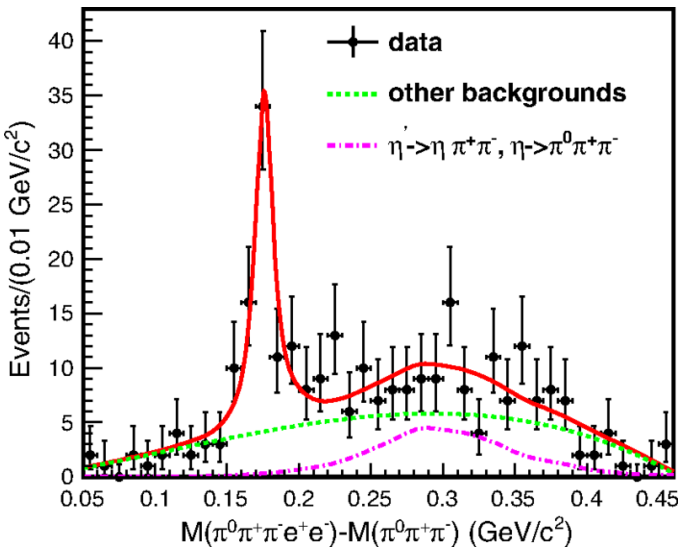

Fig. 8. Fitting results from $\eta' \to \omega e^+e^-$ on the distribution of $M(\pi^0\pi^+\pi^-e^+e^-)$–$M(\pi^0\pi^+\pi^-)$. The crosses show the distribution of data. The dash-dotted line represents the $\eta' \to \eta\pi^+\pi^-$ component, and the dotted curve shows the background except $\eta' \to \eta\pi^+\pi^-$

So for the first time, the decay of $\eta' \to \omega e^+e^-$ is observed with a statistical significance of 8 σ, and its branching fraction is measured to be $B(\eta' \to \omega e^+e^-) = (1.97 \pm 0.34(stat) \pm 0.17(syst)) \times 10^{-4}$, which is consistent with theoretical prediction, 2.0×10^{-4} [12]. The branching fraction of $\eta' \to \omega\gamma$ is determined to be $B(\eta' \to \omega\gamma) = (2.55 \pm 0.03(stat) \pm 0.16(syst)) \times 10^{-2}$, which is in good agreement with the world average value in Ref. [1] and the most precise measurement to date.

6 Summary

In summary, EM Dalitz decays could be sensitive and provide very rich information about meson structures, and plays an important role in constraining the uncertainties to $(g-2)_\mu$. BESIII has performed and published several Dalitz decays, including $\eta' \to \gamma e^+e^-$, $J/\psi \to Pe^+e^-$ ($P = \eta', \eta, and\ \pi^0$), $\eta' \to \omega e^+e^-$ etc. These processes are all observed and measured for the first time. They have furthered our knowledge about meson structures and meson interactions. Many more related work is ongoing. There will be more results to come, and they will further test the theory against the measurements and could be sensitvie to the new physics beyond the standard model.

References

1 K. A. Olive et al. (Particle Data Group), Chin. Phys. C 38, 1 (2014)
2 L. G. Landsberg, Phys. Rep. 128, 301 (1985).
3 M. Ablikim et al. (The BESIII Collaboration), Nucl. Instrum. Meth. A 614, 345 (2010)
4 M. Davier, A. Hoecker , B. Malaescu, Z. Zhang, Eur.Phys.J. C71 1515(2011); Eur.Phys.J. C72 1874(2012)
5 J. P. Miller, R. Eduardo de, B. L. Roberts, and D. Stoeckinger, Annu. Rev. Nucl. Part. Sci. 62, 237 (2012).
6 Z. R. Xu and K. L. He, Chin. Phys. C 36, 742 (2012).
7 M. Ablikim et al. (The BESIII Collaboration), Phys. Rev. D 92, 012001 (2015).
8 M. Ablikim et al. (The BESIII Collaboration), Phys. Rev. D 89, 092008 (2014).
9 M. Ablikim et al. (The BESIII Collaboration), Phys. Rev. D 92, 051101 (2015).
10 R. I. Dzhelyadin et al. (Lepton-G Collaboration), Phys. Lett. 88B, 379 (1979); JETP Lett. 30, 359 (1979).
11 J. Fu, H. B. Li, X. Qin, and M. Z. Yang, Mod. Phys. Lett. A 27, 1250223 (2012).
12 A. Faessler, C. Fuchs, M. Krivoruchenko, Phys. Rev. C 61, 035206 (2000).